

3. Results and Discussion

3.1. Characterization of photocatalysts

The characterization of pure TiO₂ and modified TiO₂ nanoparticles (photocatalysts) was achieved by different analysis methods, such as XRD, SEM, BET, FTIR and DRS after their synthesis and calcination.

The modification of TiO₂ nanoparticles with transition metal ions Pt, Pd and Ni was achieved to decrease the electron-hole recombination by trapping the electrons. Adding a low percentage of metal ions can also improve the photocatalytic activity of photocatalysts. In order to examine this effect, addition of various amounts of Pt, Pd and Ni impurities was investigated.

3.1.1. XRD patterns

The XRD patterns of TiO₂ nanoparticles are shown in Fig. 1. As it is seen, the pattern at 300°C shows

amorphous phase and do not show any crystalline phase. However, by increasing the calcination temperature to 400°C, anatase and rutile phase peaks grow. Increasing the calcination temperature caused an increase in amount of both phases. Also, the best ratio of anatase to rutile is observed at 500°C (Fig. 1). The crystalline size of TiO₂ nanoparticle was calculated from XRD patterns using scherrer equation at temperatures 400, 450, 500 and 700 °C and was 21.0, 32.0, 46.2 and 122.8 nm, respectively [1]. According to the scherrer equation, it is obvious that by increasing the temperature from 400 °C to 700 °C, the size of TiO₂ particles increases from 21.0 nm to 122.8 nm.

The XRD patterns of 0.5% Pt/TiO₂, 1% Ni/TiO₂ and 1.5% Pd/TiO₂ calcinated at 500°C are demonstrated in Fig. 2. Comparing the spectra with pure TiO₂ indicates that metallic Pt impurities has penetrated in the structure while there are no peaks for Pd and Ni.

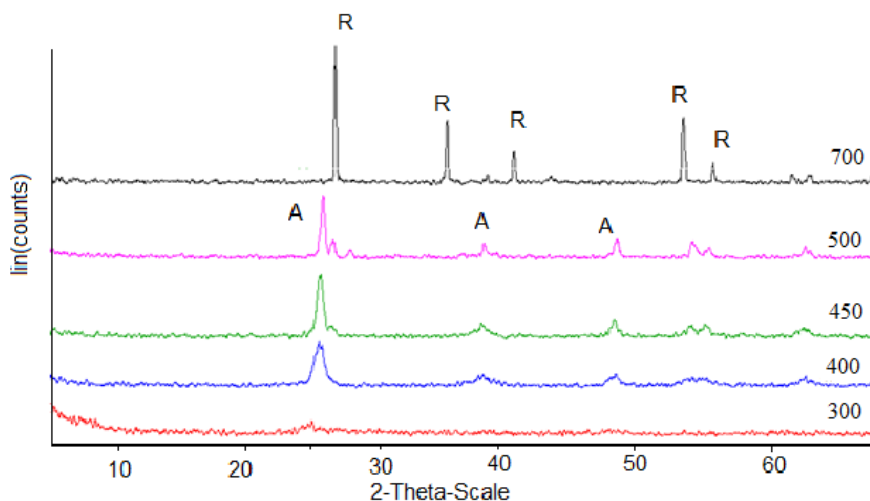


Fig. 1. XRD pattern of pure TiO₂ nanoparticles calcined at various temperatures.

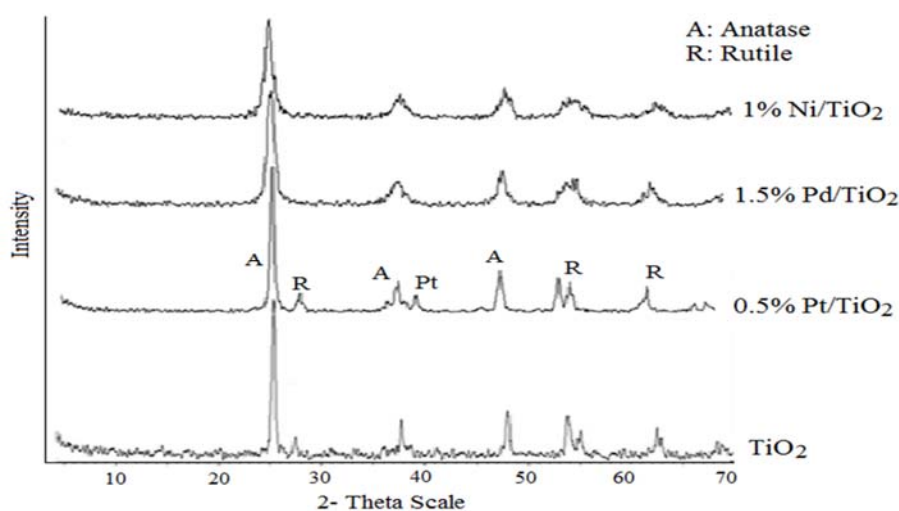


Fig. 2. XRD pattern of metal ion impregnated and bare TiO₂ photocatalysts calcinated at 500°C.

Therefore, it can be concluded that Pd and Ni are situated on surface of photocatalyst. Mean particle size of nanophotocatalysts was calculated from XRD patterns and was 37.5, 24.1 and 22.6 nm, respectively.

3.1.2. SEM analysis

Fig. 3 shows SEM micrographs of the prepared nanostructured 1% Ni/TiO₂, 1.5% Pd/TiO₂ and 0.5% Pt/TiO₂ photocatalysts that were calcinated at 500°C.

3.1.3. BET analysis

Table 1 and Table 2 give the results for BET surface area of pure TiO₂ nanoparticles calcinated at different temperatures and modified photocatalysts. It can be observed that increasing the temperature decreases the surface area. This happens because TiO₂ particles sinter at high temperature. Furthermore, the modification of TiO₂ by each transition metal causes the surface area to increase from the original value of

39.0 m² g⁻¹ to 40.5 m² g⁻¹ for 1% Ni/TiO₂, 44.8 m² g⁻¹ for 0.5% Pt/TiO₂ and 64.4 m² g⁻¹ for 1.5% Pd/TiO₂ (Table 2).

3.1.4. FT-IR spectroscopy

Fourier Transform Infrared (FT-IR) spectra of pure TiO₂ and modified TiO₂ were taken. A peak at 400-700 cm⁻¹ in all samples is attributed to Ti-O stretching vibration, which shifts to lower wavelength by adding the transition metals. A progressive red shift in the band gap adsorption is noticed with metal loading. The adsorption is associated to the charge transfer from oxygen to titanium. The spectra of TiO₂ modified with Pt have the most red-shift in comparison with the others. Thus, it can be concluded that Pt is penetrated into the structure of TiO₂ more than Pd and Ni. The IR spectra of TiO₂ modified with transition metals don't show any bands corresponding to the other transition metal oxide, which is consistent with the XRD results.

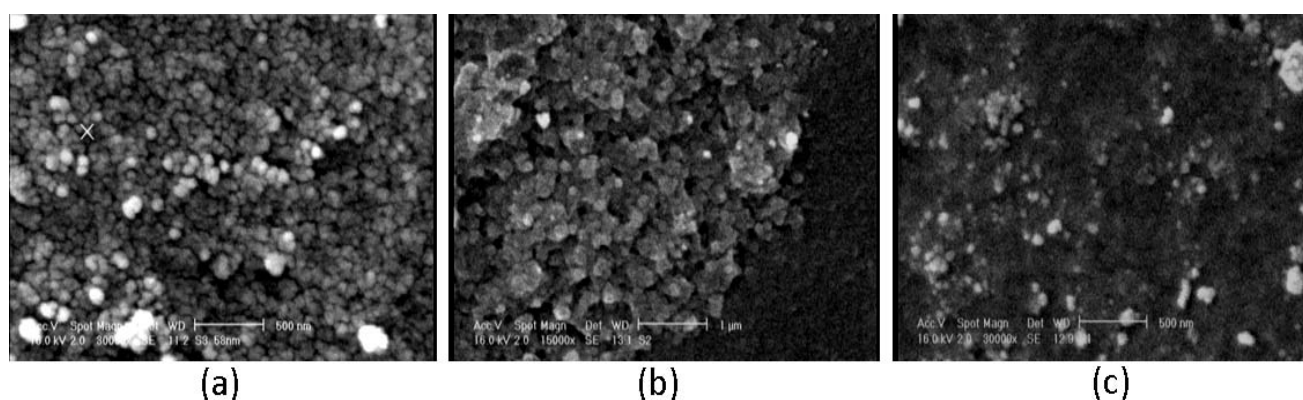


Fig. 3. SEM micrographs of: a) 0.5% Pt/TiO₂, b) 1.5% Pd/TiO₂ and c) 1% Ni/TiO₂ calcinated at 500 °C.

Table 1. BET surface area of TiO₂ nanoparticles at various calcination temperatures.

Calcination temperature (°C)	Surface area (m ² g ⁻¹)	Total pore volume (cm ³ g ⁻¹)
400	75.64	0.12
450	67.21	0.13
500	64.35	0.13

Table 2. BET surface area of metal doped TiO₂ nanoparticles.

Catalyst	Mean pore diameter (nm)	Surface area (m ² g ⁻¹)	Total pore volume (cm ³ g ⁻¹)
TiO ₂	10.20	39.0	0.90
1% Ni/TiO ₂	84.90	40.5	0.08
0.5% Pt/TiO ₂	80.14	44.8	0.16
1.5% Pd/TiO ₂	94.70	64.4	0.13

3.1.5. DRS analysis

The band gap energy of the catalysts is determined using DRS (Diffuse Reflectance Spectra). A spectrophotometer equipped with an integrating sphere, and Barium Sulfate is used as a reference. The spectra are recorded at room temperature for $350 < \lambda < 800$ nm. The energy band gaps of catalysts are calculated according to the Eq. (1).

$$E_g = hc/\lambda \quad (1)$$

Where E_g , h , c and λ are the energy band gap (eV), Planck's constant, the light velocity (m/s) and the wavelength (nm), respectively. DRS results show the effect of transition metals on band structure and energy band gap. UV light absorption for TiO_2 appears at 372 nm in DRS spectra. This absorption is associated with the charge-transfer from oxygen to titanium whose electrons are excited and transferred from the valence band to the conduction band. The observable shifts of the absorbance edge to the visible light region are detected for modified TiO_2 (Table 3). These results show that small amounts of the dopants might be incorporated into the lattice of TiO_2 . When transition metal ions are incorporated into the lattice, levels of dopants appear between the valence band and the conduction band, the energy band gap alters and the absorbance edge shifts to the visible light region.

3.2. Kinetic investigation and the mechanism of photocatalytic oxidation

In the photocatalytic process, the efficiency of photooxidation of DMMP at different sampling times is calculated from the Eq. (2).

$$Efficiency (\%) = [(C_0 - C)/C_0] \times 100 \quad (2)$$

Here, C_0 is the initial solution concentration and C is the solution concentration after the reaction time. The photocatalytic oxidation of DMMP follows the first-order decay kinetic. Previous studies show that photocatalytic oxidation rate of the most organic compounds, which are in heterogeneous photocatalytic oxidation systems and under UV-light illumination, obey the Langmuir-Hinshelwood (L-H) kinetics model [1,18,19].

Table 3. The results of DRS analysis of photocatalysts.

	TiO_2	Ni/ TiO_2	Pd/ TiO_2	Pt/ TiO_2
λ (nm)	372	387	403	558
E_g (eV)	3.3	3.2	3.0	2.2

$$r = dc/dt = kKC/(1 + KC) \quad (3)$$

In this equation r , C , t , k and K are oxidation rate ($mol L^{-1} min^{-1}$), concentration of the reactant ($mol L^{-1}$), illumination time (min), reaction rate constant (min^{-1}) and adsorption coefficient of the reactant ($L mol^{-1}$) respectively. For low initial DMMP concentrations (when C_0 is small), the rate is proportional to the substrate concentration. In this case, the rate constant is observed to be the pseudo-first order [1]. Therefore, the Eq. (3) can be changed to Eq. (4).

$$Ln(C/C_0) = kKt = k_{app}t \quad (4)$$

Fig. 4 shows the linear behavior of the values calculated from Eq. (4) for palladium containing the catalyst with $R^2 = 0.969$, which confirms the pseudo-first order reaction. In addition, the apparent rate constant can be calculated from the slope. According to the results, the following mechanism for the oxidation of DMMP on the surface of photocatalyst can be proposed [1,3,9]. Absorbed photons by photocatalysts causes the generation of electron-hole pairs which initiate the photodegradation process. These agents are able to produce superactive radicals like hydroxide ones which attack the organic compounds in the medium and destroy them (Fig. 5). As a result, whatever can delay the electron hole recombination, enhances the concentration of the radicals and the photocatalytic efficiency.

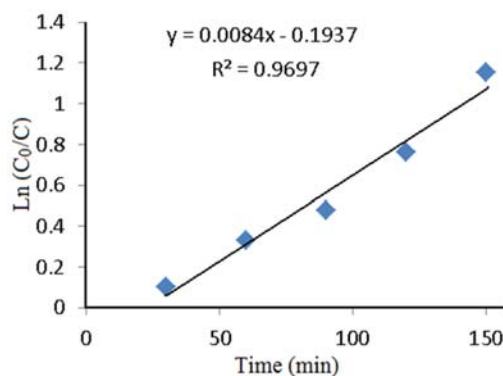
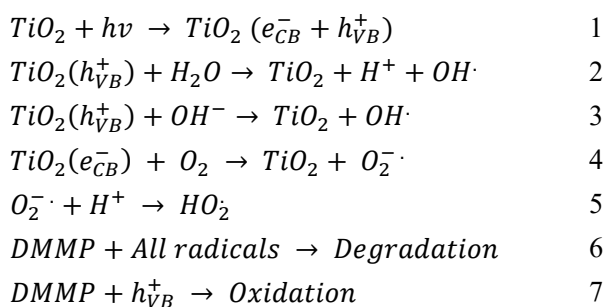


Fig. 4. The photodegradation of DMMP with 1% Pd/ TiO_2 after treatment time.

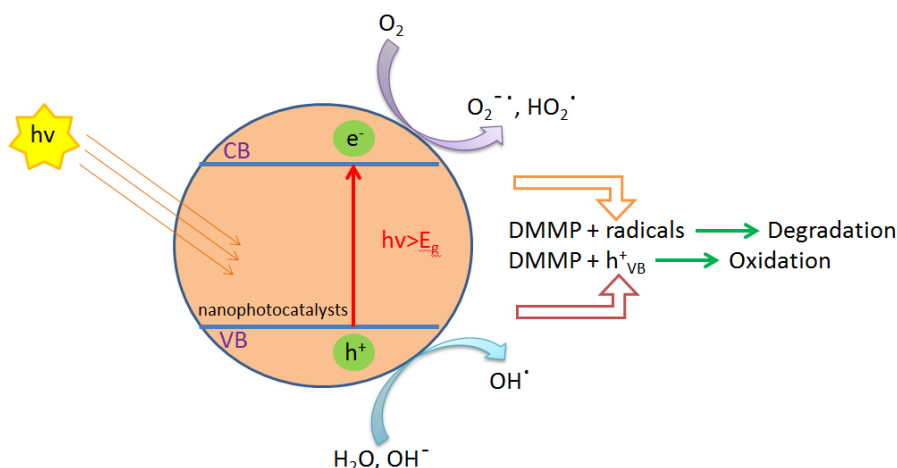


Fig. 5. Mechanism of photocatalytic action of TiO₂ nanocatalysts under UV light irradiation.

3.3. The mechanism of transition metal effect on TiO₂ photocatalytic activity

The effect of the type (Pt, Pd and Ni) and amount (0.5, 1.0 and 1.5%) of loading transition metals on the photocatalytic efficiency are shown in Fig. 6 and 7. As can be seen in these figures, the best photooxidation of DMMP was obtained with 1% Pd/TiO₂.

Modified TiO₂ photocatalysts have a higher photoactivity than pure TiO₂. Adding transition metals to the TiO₂ surface can enhance the efficiency of photocatalytic oxidation. Because, the modified TiO₂ particles have a lower crystal size, higher surface area, higher efficiency for the electron-hole regeneration, and higher charge trapping. The charge trapping can be demonstrated by the following equations [1,33].



The holes can transfer to the surface of TiO₂ and react with species in solution (O₂ or hydroxide) to produce the oxidant radicals. When Ti ions of TiO₂ are replaced by transition metal ions, the most of dopant levels appear between the valence band and the conduction band, which can increase the rate of surface trapping of carrier and retard the electron-hole recombination. Therefore, the efficiency of photocatalytic oxidation is enhanced.

3.4. The effect of catalyst dosage

The effect of the photocatalyst dosage on the photooxidation of DMMP solution was studied and the results are presented in Fig. 8. The photocatalytic activities can be related to the availability of active sites on the photocatalyst surface [33]. For 1% Pd/TiO₂, the photo oxidation efficiency is enhanced up to 20 g L⁻¹ of the catalyst dosage and then it decreases. The addition of an extra amount of photocatalyst can increase the amount of DMMP absorbed and the number of active catalytic sites for its degradation.

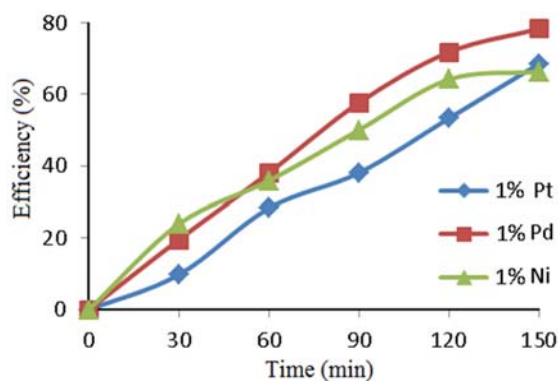


Fig. 6. The effect of type of the loaded metal on the photocatalytic efficiency (DMMP: 0.092 M, catalyst dosage: 10 g L⁻¹, temperature: RT).

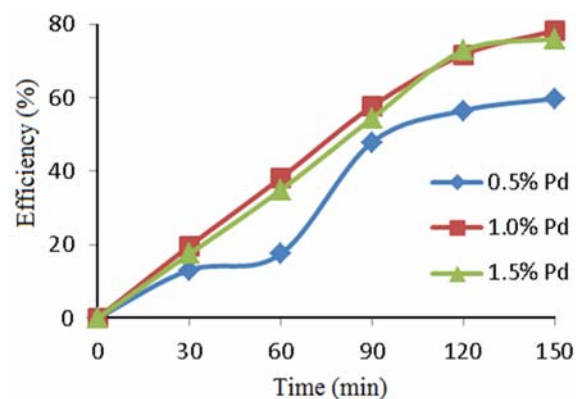


Fig. 7. The effect of the amount of loading metal on the photocatalytic efficiency (DMMP: 0.092 M, catalyst dosage: 10 g L⁻¹, temperature: RT).

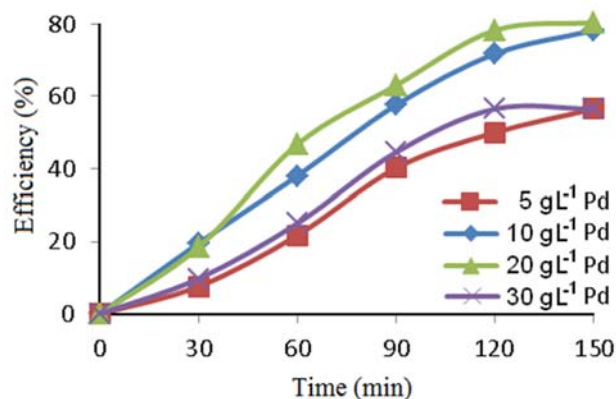


Fig. 8. The effect of catalyst dosage on the photocatalytic oxidation of DMMP (DMMP: 0.092 M, temperature: RT).

However, if the catalyst concentration reaches a specific value, the photooxidation efficiency decreases for different reasons such as agglomeration, light-scattering, and sedimentation of catalyst particles [1,8].

3.5. The effect of initial concentration of DMMP

The effect of the initial DMMP concentration on the photooxidation rate and efficiency is shown in Fig. 9. It was observed that the photooxidation efficiency increases with an increase in the initial concentration of DMMP until 0.138 M at first, and then it decreases. This may be attributed to the fact that the active sites of the catalyst are covered by the organic compound present at high concentration and, therefore, a significant amount of UV light may be absorbed by the organic molecules rather than by the catalyst particles [26]. Thus, the generation of oxidant radicals on the surface of catalysts is reduced and the efficiency of DMMP photooxidation is decreased.

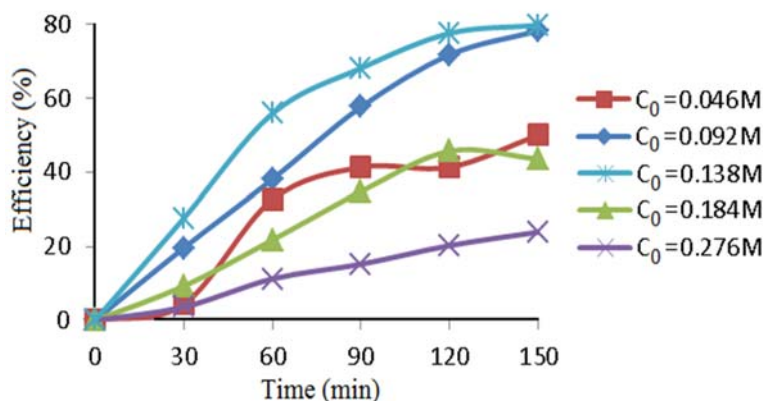


Fig. 9. The effect of initial DMMP concentration on the photocatalytic oxidation of DMMP (catalyst dosage: 10 g L⁻¹, temperature: RT).

4. Conclusion

TiO₂ based photocatalysts modified with transition metals Pt, Pd and Ni were synthesized by sol-gel method. The prepared photocatalysts were characterized by different analysis methods such as XRD, FTIR, SEM, DRS and BET. The photocatalytic properties of the prepared samples were evaluated by photooxidation of DMMP as an organophosphorus simulant of chemical warfare agent. A kinetic and mechanistic study was performed and the photocatalytic oxidation of DMMP with palladium containing the catalyst followed the pseudo first-order decay kinetic. The effects of some parameters such as photocatalyst dosage, initial concentration of DMMP and the amount and type of loading impurities on the photocatalytic efficiency were studied. The results showed that the best photoactivity was obtained with

1% Pd/TiO₂. According to the results, at first, the photooxidation efficiency increased with an increase in the catalyst dosage and initial concentration of DMMP and then it decreased.

References

- [1] S. Ghasemi, S. Rahimnejad, S. Rahman Setayesh, S. Rohani, M.R. Golami, J. Hazard. Mater. 172 (2009) 1573-1578.
- [2] R.J. Tayade, R.G. Kulkarni, R.V. Jasro, Ind. Eng. Chem. Res. 45 (2006) 5231-5238.
- [3] C. Dominguez, J. Garcia, M.A. Pedraz, A.A. Torres, M.A. Galan, Catal. Today 40 (1998) 85-101.
- [4] M.H. Habibi, E. Askari, Iran. J. Catal 1 (2011) 41-44.
- [5] H. Faghian, A. Bahrani, Iran. J. Catal 1 (2011) 45-50.
- [6] H.R. Pouretedal, S. Basati, Iran. J. Catal. 2 (2012) 51-55.

- [7] H.R. Pouretedal, M. Ahmadi, Iran. J. Catal. 3 (2013) 149-155.
- [8] S. Malato, J. Blanco, A.R. Fernández-Alba, A. Agüera, Chemosphere 40 (2000) 403-409.
- [9] J.P. Percherancier, R. Chapelon, B. Pouyet, J. Photochem. Photobiol. A 87 (1995) 261-266.
- [10] R.A. Doong, W.H. Chang, J. Photochem. Photobiol. A 107 (1997) 239-244.
- [11] M. Kerzhentsev, C. Guillard, J.M. Herrmann, P. Pichat, Catal. Today 27 (1996) 215-220.
- [12] M. Arami, N. Yousefi Limaee, N.M. Mahmoodi, N. Salman Tabrizi, J. Hazard. Mater. 135 (2006) 171-179.
- [13] S. Gautam, S.P. Kamble, S.B. Sawant, V.G. Pangarkar, Chem. Eng. J. 110 (2005) 129-137.
- [14] S. Malato, J. Blanco, M.I. Maldonado, P. Fernandez-Ibanez, A. Campos, Appl. Catal. B 28 (2000) 163-174.
- [15] A.L. Linsebigler, G. Lu, J.T. Yates, Chem. Rev. 95 (1995) 735-758.
- [16] M. Kaneko, I. Okura, Photocatalysis, Science and Technology, Springer, Germany, 2002.
- [17] A. Hagfeldt, M. Graetzel, Chem. Rev. 95 (1995) 49-68.
- [18] P.V. Kamat, Chem. Rev. 93 (1993) 267-300.
- [19] N. Serpone, E. Pelizzetti, Photocatalysis: Fundamentals and Application”, John Wiley & Sons, New York, 1989.
- [20] A. Mills, S. Le Hunts, J. Photochem. Photobiol. A 108 (1997) 1-35.
- [21] M.A. Fox, M.T. Dulay, Chem. Rev. 93 (1993) 341-357.
- [22] W.Y. Ching, J. Am. Ceram. Soc. 73 (1990) 3135-3159.
- [23] M.S. Ahmed, Y.A. Attia, J. Non-Cryst. Solids 186 (1995) 402-407.
- [24] G. Balasubramanian, D.D. Dionysiou, M.T. Suidan, Dekker Encyclopedia of Nanoscience and Nanotechnology, Vol. 6, Marcel Dekker Inc., New York, 2004.
- [25] J. Hagen, Industrial Catalysis: A Practical Approach, 2nd Ed., John Wiley & Sons, Germany, 2006.
- [26] I.K. Komstantinou, T.A. Albanis, Appl. Catal. B 49 (2004) 1-14.
- [27] Y. Ishibai, J. Sato, T. Nishikawa, S. Miyagishi, Appl. Catal. B 79 (2008) 117-121.
- [28] J.M. Kwon, Y.H. Kim, B.K. Song, S.H. Yeom, B.S. Kim, J.B. Im, J. Hazard. Mater. 134 (2006) 230-236.
- [29] E. Bizani, K. Fytianos, I. Poullos, V. Tsiridis, J. Hazard. Mater. 136 (2006) 85-94.
- [30] S.L. Bartelt-Hunt, D.R.U. Knappe, M.A. Barlaz, Crit. Rev. Env. Sci. Tech. 38 (2008) 112-136.
- [31] A. Besharati-Seidani, M.R. Gholami, Iran. Chem. Chem. Eng. J. 34-1 (2015) 39-49.
- [32] M. Padervand, M. Tasviri, M.R. Gholami, Chem. Papers 65 (2011) 280-288.
- [33] M.N. Rashed, A.A. El-Amin, Int. J. Phys. Sci. 2 (2007) 73-81.